JHR 90: 129–152 (2022)
doi: 10.3897/jhr.90.75807
https://jhr.pensoft.net

RESEARCH ARTICLE

JOURNAL OF Hymenoptera RESEARCH
A peer-reviewed open-access journal
The International Society of Hymenopterists

Integrative taxonomy based on morphometric and molecular data supports recognition of the three cryptic species within the *Encyrtus sasakii* complex (Hymenoptera, Encyrtidae)

Andrey Rudoy[1], Chao-Dong Zhu[1,2,3], Rafael R. Ferrari[1], Yan-Zhou Zhang[1]

1 *Key Laboratory of Zoological Systematics and Evolution, Institute of Zoology, Chinese Academy of Sciences, 1 Beichen West Road, Chaoyang District, Beijing 100101, China* **2** *University of Chinese Academy of Sciences, 19A Yuquan Road, Shijingshan District, Beijing 10049, China* **3** *State Key Laboratory of Integrated Pest Management, Institute of Zoology, Chinese Academy of Sciences, 1 Beichen West Road, Chaoyang District, Beijing 100101, China*

Corresponding author: Yan-Zhou Zhang (zhangyz@ioz.ac.cn)

Academic editor: Petr Janšta | Received 28 September 2021 | Accepted 16 March 2022 | Published 29 April 2022

http://zoobank.org/52BFC574-91CC-472E-AB4B-0095DEE349A0

Citation: Rudoy A, Zhu C-D, Ferrari RR, Zhang Y-Z (2022) Integrative taxonomy based on morphometric and molecular data supports recognition of the three cryptic species within the *Encyrtus sasakii* complex (Hymenoptera, Encyrtidae). Journal of Hymenoptera Research 90: 129–152. https://doi.org/10.3897/jhr.90.75807

Abstract

Morphometrics has established itself as one of the most powerful tools for species delimitation, particularly for morphologically-conserved groups of insects. An interesting example is the parasitoid *Encyrtus sasakii* Ishii (Hymenoptera: Chalcidoidea: Encyrtidae), which was recently subdivided into three cryptic species that are seemingly well-delimited with the available DNA data but nearly indistinguishable morphologically. Here, we performed linear morphometric analyses of the antenna as well as shape analyses of the ovipositor and hypopygium (the last two are key structures associated with host location and selection) to shed further light on the taxonomic status of the *E. sasakii* complex. Principal component analyses were carried out to visualize the amount and direction of shape variation in the ovipositor and hypopygium. Complementarily, we constructed phylogenetic trees using a Bayesian approach based on two markers (28S and COI). We found statistically-significant differences in the relative size of the funicle and of the two proximal claval antennomeres among the three species. Our analyses also indicated that the outer plates of the ovipositor show remarkable allometric changes and that both the stylus and shield of the ovipositor are relatively well conserved among species. We nonetheless found consistent interspecific differences in the shape of the 2nd outer plate of the ovipositor and hypopygium. Also, both our COI and combined trees recovered three strongly-supported major clades, each corresponding to one of the three cryptic species. We discuss that changes in the shape of the ovipositor may have played an important role in host shift and speciation within

the *E. sasakii* complex. Even though the recent descriptions of both *E. eulecaniumiae* Wang & Zhang, 2016 and *E. rhodococcusiae* Wang & Zhang, 2016 appear not to fully satisfy the International Code of Zoological Nomenclature, a simple resolution for the sake of taxonomic stability is proposed herein.

Keywords
Allometry, Chalcidoidea, DNA barcoding, morphometrics, parasitoid, species delimitation

Introduction

Cryptic species are phylogenetically closely-related ones that exhibit no unambiguous morphological differences to readily permit their distinction (Tan et al. 2010; Pramual et al. 2011; Lukhtanov 2019). This understanding has led researchers to use additional lines of evidence – such as behavior (Vodă et al. 2015), physiology (Allemand 1982) and ecology (Amato et al. 2007) – as an attempt to more reliably identify cryptic species (Dépraz et al. 2009; Orr et al. 2020). Obtaining such kind of data, however, requires either observation in field or experimentation with laboratory-reared animals, which is usually impeditive for most groups of organisms (Milne et al. 2007). Thus, the use of tree inference methods in combination with DNA data (which can today be obtained from fairly-old museum specimens) has arguably become the most popular approach for cryptic species identification (e.g., Padula et al. 2016; Delicado et al. 2019), especially after the onset of the 'DNA barcoding' era (Hebert et al. 2003a, b). In spite of important advances in the field of molecular taxonomy (see Gokhman 2018), comparative morphology indisputably remains as a reliable approach to species identification and delimitation within Hymenoptera (e.g., Zhang et al. 2014; Monckton 2016; Ferrari 2017; Nugnes et al. 2017; Hasson and Schmidt 2020).

Morphological taxonomists have been adopting multiple different approaches as an attempt to better solve the puzzling problem of cryptic species. A notable one has been inferring gaps in the morphological variation exhibited by closely-related species across their geographical ranges (Zapata and Jiménez, 2011). However, it has been demonstrated that continuous variation may be interrupted by factors that are not necessarily associated with diversification (Viggiani 1999), meaning that discontinuity is not always an evidence for speciation (Gutiérrez-Valencia et al. 2017). Another popular approach for cryptic-species delimitation is geometric morphometrics, which is based on statistical analyses of landmark data (Sproul and Maddison 2017). Morphometric studies have largely relied on two premises: first, allometric changes arise from directional and non-symmetrical selection of morphological traits (Pomfret and Knell 2006), including non-sexual ones (Frankino et al. 2007); second, such selection ultimately leads to speciation (Soto et al. 2007). Intraspecific allometry may be associated with either environmental (Klingenberg and Zimmermann 1992) or genetic factors (Trotta et al. 2010), although a combination of the two appears more likely.

Both the antenna and the ovipositor apparatus are structures of singular taxonomic relevance for parasitoid wasps. Females utilize the former as a chemical radar to search

for hosts in the environment (Broad and Quicke 2000). This structure is also used by both sexes for intraspecific recognition during copulation (Arbuthnott and Crespi 2018). This makes the antenna vital not only for the reproduction of parasitoid wasps, but ultimately for their environmental adaptation (Fea et al. 2019). As a result, selective pressures have produced a myriad of different antennal forms (Krishnan and Sane 2015), which can be used as frameworks to understand the diversity of parasitoid wasps across different hierarchical scales. Female parasitoids use the ovipositor to locate and lay eggs inside their hosts (Vinson 1998). It is known that host specialization, including changes in the egg-laying behavior, plays an important role in the evolution of the ovipositor in parasitoids (Ghara et al. 2011; Desneux et al. 2012). Morphological changes in this key structure, in turn, may result in prezygotic barriers for conspecific populations (Rull et al. 2013). In fact, host specialization has been pointed out as a major driver of speciation in parasitoid wasps (Zhang et al. 2011; Chesters et al. 2012; Qin et al. 2018).

The *Encyrtus sasakii* Ishii complex comprises three parasitoid species (*E. sasakii*, *E. eulecaniumiae* Wang & Zhang and *E. rhodococcusiae* Wang & Zhang) of coccoid scale insects (Wang et al. 2016). While *E. sasakii* was described almost a century ago (Ishii 1928), both *E. eulecaniumiae* and *E. rhodococcusiae* were only recently identified (Chesters et al. 2012) and then formally described (Wang et al. 2016). All three species are seemingly endemic to China and Japan: *E. eulecaniumiae* and *E. rhodococcusiae* occur sympatricly while *E. sasakii* is allopratic in relation to the other two (see Wang et al. 2016: Suppl. material 1: Fig. S3), although no impassible geographic barriers separating them seem to exist.

Species of the *E. sasakii* complex are almost indistinguishable when only traditional morphological methods are used (Chesters et al. 2012). They are nonetheless significantly divergent according to the available molecular data, which showed that *E. sasakii* and *E. rhodococcusiae* are more closely related with each other than either of them is in relation to *E. eulecaniumiae* (Wang et al. 2016). Laboratory-reared individuals did not exhibit any interspecific courtship and mating behavior during controlled experiments, which further supported the view that they should be treated as different species. However, linear morphometric analyses carried out by the same authors did not detect any unambiguous morphological differences among the three species to support their molecular data (Wang et al. 2016). Thus, the main objective of this paper is to shed further light on the taxonomic status of the encyrtid species of the *E. sasakii* complex through an integrative approach to taxonomy. Specifically, we present the results of phylogenetic analyses of two molecular markers and morphometric analyses of the antenna, ovipositor and hypopygium of females and discuss their taxonomic implications.

Methods

Specimens examined

The material examined includes recently collected specimens plus part of those studied previously by Wang et al. (2016). All specimens (including all types) are deposited in

the entomological collection of the Institute of Zoology, Chinese Academy of Sciences, Beijing, China (IZCAS). Additional collection data are given in Suppl. material 1: Table S1.

Analysed structures and imaging

This study is based on morphometric analyses of the antenna, ovipositor and hypopygium of female parasitoids (Fig. 1A–C). Funicular and claval antennomeres are herein abbreviated as F and C, respectively, followed by appropriate number (for example, F1 for the first funicular antennomere). All analysed structures were dissected from previously-relaxed specimens using fine-tipped forceps and then mounted onto microscopy slides in Canada balsam. Digital images of slide-mounted structures were obtained with a Leica DM 2500 microscope equipped with a Canon EOS 550D camera, using a magnification of 100× (except the forewing that was imaged with a magnification of

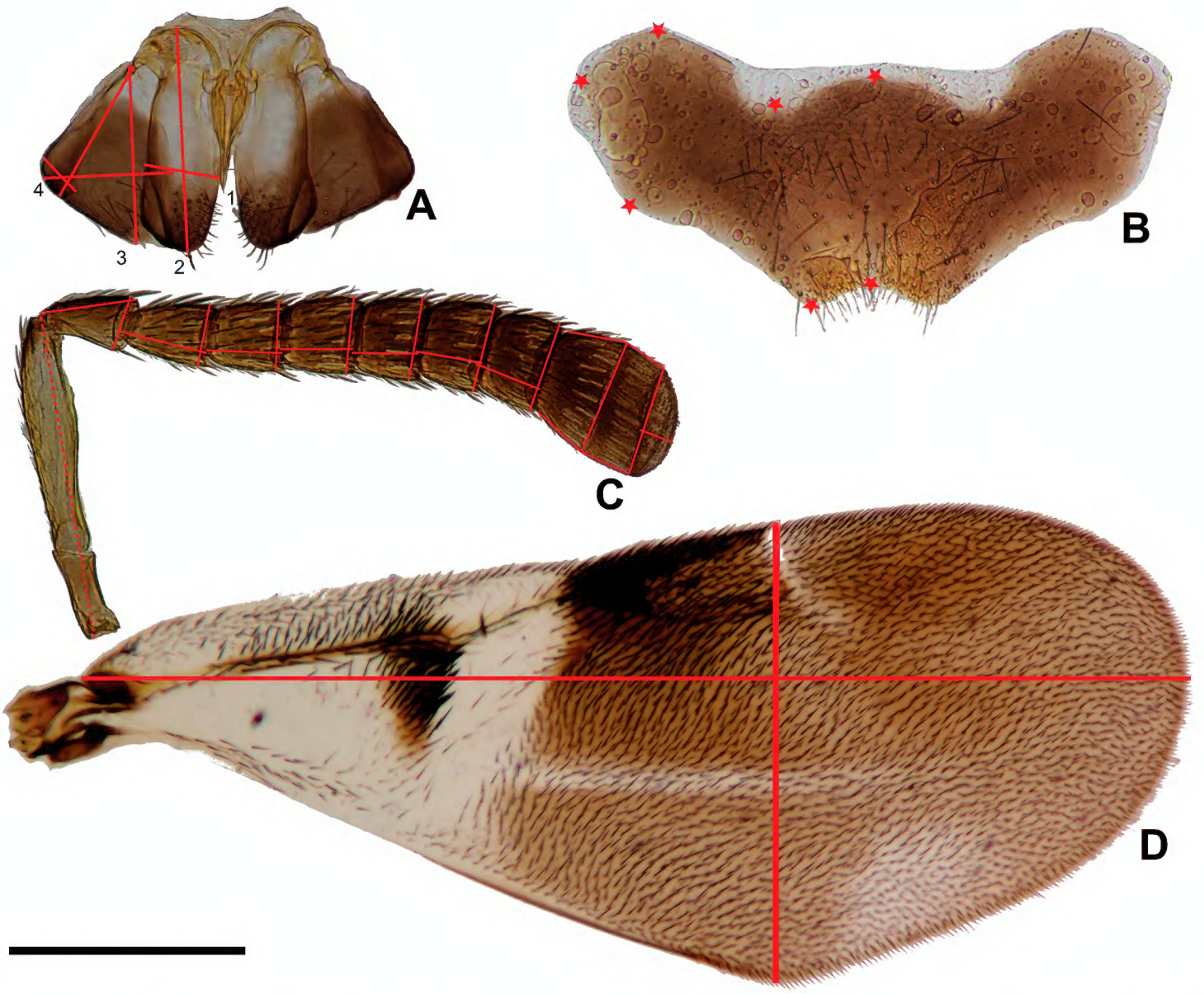

Figure 1. Indications as to how structures were measured (red lines) and fixed landmarks defined (red stars) **A** ovipositor of *E. eulecaniumiae* (1 – stylus, 2 – ovipositor shield, 3 – 1st outer plate, 4 – 2nd outer plate) **B** hypopygium of *E. rhodococcusiae* **C** antenna of *E. rhodococcusiae* **D** wing of *E. eulecaniumiae*. Scale bar: 400 μm.

50×). For each structure, 10 to 20 photographs were taken and then stacked together to produce multifocus images using the program Helicon Focus v.3.10.3.

In *Encyrtus*, the funicle comprises six well-delimited antennomeres (F1–F6), while the clava consists of three (C1–C3) nearly-fused ones (Fig. 1C). The ovipositor typically has the same general shape (Figs 1A, 2A–D), exhibiting no clear structural differences within the genus. The stylus (Fig. 2A) forms the central axis of the ovipositor and is composed of the 1st and 2nd valvulae that are firmly connected to one another. The 3rd valvula (gonostylus) and 2nd valvifer are completely fused in *Encyrtus* and together they form the ovipositor shield (Fig. 2B), which surrounds the stylus laterally. The 1st valvifer, which is connected to the 2nd valvifer and both outer plates basally (Noyes 2010), was not included in our morphometric analyses due to the absence of well-delimited margins. Here, the 2nd outer plate refers to the ventrally-oriented, subtriangular structure that is somewhat loosely connected to the external margin of the 1st outer plate (Fig. 2C, D). The hypopygium consists of the seventh metasomal sternite (Fig. 1B).

Measurements and linear morphometrics

Image files were imported in ImageJ v. 1.8 (National Institutes of Health; available at http://imagej.nih.gov/ij/), where the measurements used in our linear morphometric

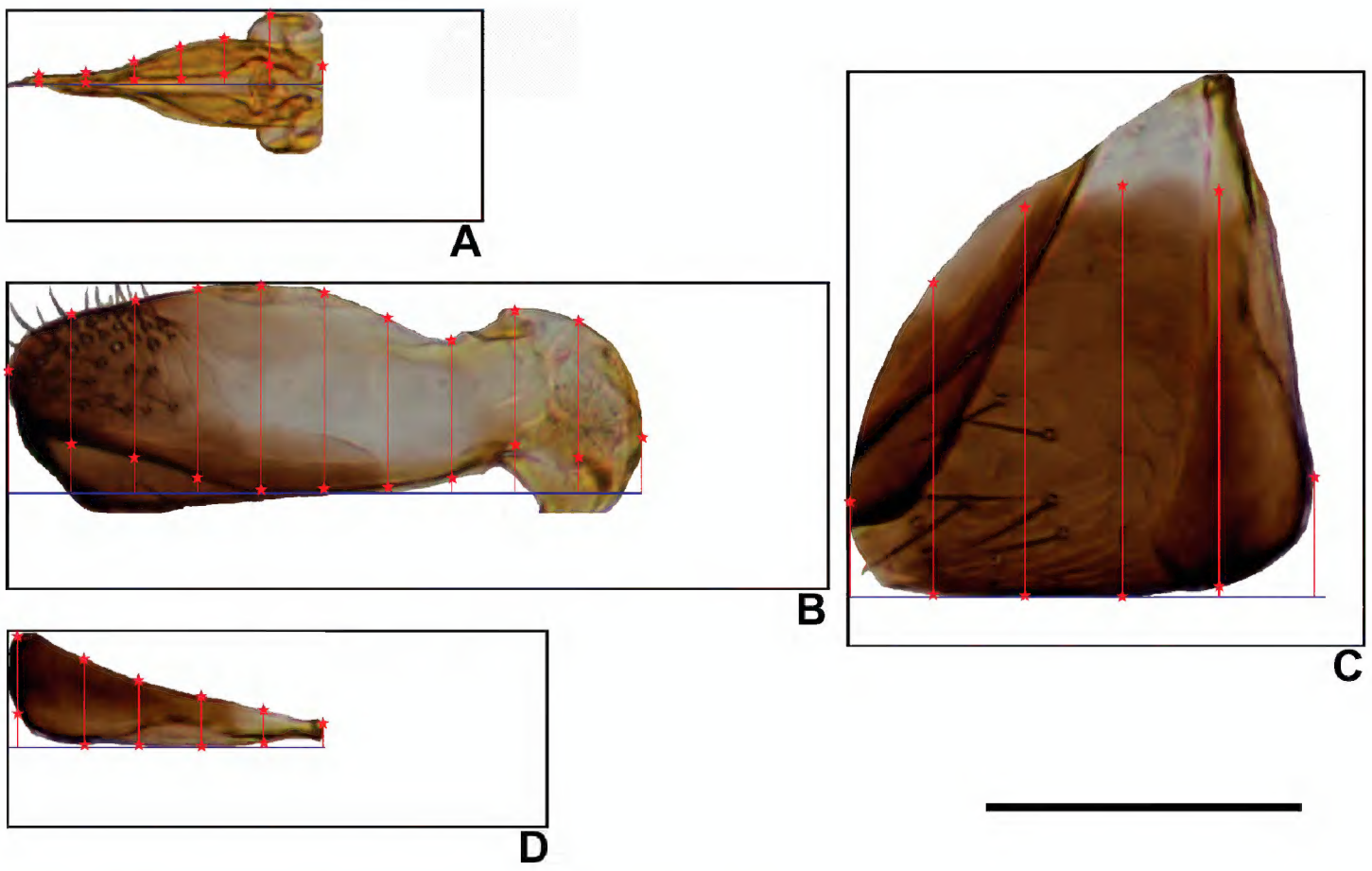

Figure 2. Indication as to how semi-landmarks (red stars) were marked on the various components of the ovipositor **A** stylus (1st and 2nd valvulae) **B** shield (1st and 2nd valvifers) **C** 1st outer plate **D** 2nd outer plate. Blue and red lines depict reference baselines and distances to them from the landmarks, respectively; black rectangles represent the structures prior to size transformation. Scale bar: 400 micrometers.

analyses were obtained. To minimize errors, all measurements were repeated twice and the resulting averages were then used as input values.

In this paper, forewing length was used as a proxy for body size based on preliminary analyses and previous entomological studies (e.g., DeVries et al. 2020; Wonglersak et al. 2020). The forewing was measured as the distance between the basal point of the wing membrane and the tip of the wing; its maximum width was measured through the perpendicular line connecting the apexes of the postmarginal vein and posterior margin of the forewing (Fig. 1D). The total length of the antennal clava was obtained by summing up the maximum lengths of each of its three antennomeres; its maximum width was measured along the sulci that separate the claval antennomeres (Fig. 1C). Following Wang et al. (2016), we calculated the total length of the funicle as the sum of the length of each funicular antennomere, using the sensilla as a reference point; the maximum width of the funicle was taken as the width of its distalmost antennomere (i.e., F6). The length of the pedicel was taken as the maximum distance between its articulation with the scape and its upper margin. The scape was measured as the distance between its lower margin (near the antennal socket, i.e., including the radicle) and its articulation with the pedicel. All measurements were obtained from the dorsal surfaces of the antennal parts, except the clava, which was measured from both the dorsal and ventral surfaces. The total length of the antenna was then calculated as the sum of the lengths of the clava (dorsal surface only), funicle, pedicel and scape (Fig. 1C). The total length of each analysed component of the ovipositor was measured as the distance between their anterior- and posteriormost sclerotized parts; their maximum width was taken through the perpendicular line connecting their inner- and outermost sclerotized parts (Fig. 2A–D).

As the antennomeres of the three studied species of *Encyrtus* have well-conserved shapes, they were not included in our shape analyses (*vide infra*). Rather, we carried out statistical analysis of variance (ANOVA) using the Rcmdr package (Fox 2005) in the program R (R Core Team 2019) to see whether there was significant difference in the length, width and corresponding length/width ratio (henceforth LW ratio) of each antennal antennomere. Additionally, we calculated the slope of regression of the LW ratio of each antennal antennomere. The aforementioned test was also carried out with each part of the ovipositor separately.

Shape analyses

We performed shape analyses of the hypopygium (Fig. 1B) and ovipositor (Fig. 2A–D). Prior to landmarks digitalization, we generated separate image files for the stylus, shield, and 1st and 2nd outer plates of the ovipositor using the previously-obtained pictures of the entire ovipositor. The images were then converted to the same size (500, 750 and 1,000 pixels for both the stylus and 2nd plate of the ovipositor, 1st plate of the ovipositor and ovipositor shield, respectively) while maintaining their original proportions (Fig. 2A–D) in the program PAST v.3.2 (Hammer et al. 2001). To ensure homology among the landmarks set subsequently, we fixed the images of the ovipositor into the

same position using the following well-defined reference points: central axis of stylus; connection between the 1st valvifer and the lateralmost point of the ovipositor shield; two points of the apical edge of the outer plate; connection between the 1st valvifer and the lateralmost point of the 2nd outer plate. The images of the hypopygium were fixed based on its well-defined lateral concavities.

We used ImageJ to digitalize seven fixed landmarks on the hypopygium (Fig. 1B) and 54 semi-landmarks on the ovipositor (Fig. 2A–D); the latters were distributed as follows: stylus (n = 11, Fig. 2A), ovipositor shield (n = 20, Fig. 2B), 1st outer plate (n = 10, Fig. 2C) and 2nd outer plate (n = 13, Fig. 2D). The number of semi-landmarks varied according to the shape complexity of each ovipositorial component. More specifically, we marked equidistantly distributed points along the reference levels, covering the outlines of all structures entirely, except for the often crumpled apex of the 2nd outer plate. However, the soft tissue surrounding more strongly-sclerotized parts of both ovipositor and hypopygium were not considered. The selected landmarks were superimposed using the Procrustes method (Rohlf 1990) in PAST to minimize the influence of size and position on subsequent analysis. We then performed evolutionary and ordinary principal component (EPC and PC, respectively) analyses to visualize the amount and direction of shape variation in the ovipositor. EPC analysis was carried out to control for the influence of phylogenetic inertia on our morphometric data, using a newly-constructed Bayesian tree as input (*vide infra*).

Correlation analyses

We performed ordinary correlation analyses in PAST and used the PDAP: PDTREE package v.1.15 (Midford et al. 2010) available in Mesquite 3 (Maddison and Maddison 2019) for phylogenetically constrained correlation analyses. Logarithm-transformed values of the following measurements were used in the calculation of allometry coefficients: (i) width and total length of the antenna; (ii) length and width of each funicular antennomere separately; (iii) length and width of all studied components of the ovipositor; (iv) and forewing length. We tested for correlation among the shape parameters of each component of the ovipositor and hypopygium using evolutionary and ordinary principal components. We also carried out ANOVA analyses to test for the significance of the slopes of regression among species.

DNA dataset and phylogenetic inference

The DNA dataset employed in this study consisted of partial sequences of two loci: 28S rDNA large subunit (28S) and cytochrome *c* oxidase subunit I (COI). Most of the sequences of both 28S (56 of 87, *c.* 64%) and COI (59 of 87, *c.* 68%) were originally generated by Chesters et al. (2012) and obtained from GenBank; the remaining sequences were newly generated (see Suppl. material 1: Table S1). Field collected parasitoids were euthanized with 95% ethanol and then stored at -20 °C freezer until further processing. DNA extraction, amplification and sequencing were then performed

through the protocols outlined in Chester et al. (2012). To cancel the well-known problem associated with missing data (see Wiens 2003), we only added to our phylogenetic analysis the terminals for which both 28S and COI sequences were available.

The obtained sequences of 28S and COI were pooled within two separate sequence blocks, which were then aligned separately in BioEdit v.7.04.1 (Hall 1999) using the ClustalW algorithm (Thompson et al. 1994). The resulting alignments were visually inspected and any obvious misalignments manually corrected. The longest sequences of each block were trimmed so that all regions were present in most samples. The two individual blocks (28S = 566 bp, COI = 601 bp) were concatenated in Mesquite resulting in a single multilocus matrix of 1167 bp in length.

In total, we conducted three Bayesian phylogenetic analyses with our molecular dataset: two separate single-locus analyses (28S and COI) and one multilocus analysis. In all cases, 87 terminals were included, 75 of which belonging to the *E. sasakii* complex (ingroup). The remaining 12 terminals were outgroups belonging to three different species, namely: *E. aurantii* (Geoffroy, 1785) (four terminals), *E. infelix* (Embleton, 1902) (five terminals) and *E. infidus* (Rossi, 1790) (three terminals). The analyses were performed remotely in CIPRES Science Gateway (Miller et al. 2011) using MrBayes v.3.2.6 (Huelsenbeck and Ronquist 2001; Ronquist et al. 2012). First, we used PartitionFinder v.2.1.1 (Lanfear et al. 2017) to choose the best partitioning scheme and model(s) of nucleotide substitution for our data, using the Bayesian Information Criterion and "greedy" option. The following partition and models were determined by PartitionFinder and then implemented in the phylogenetic analyses: 28S – single partition (SYM + I + Γ); COI – 1st and 2nd codons (GTR + I + Γ), 3rd codon (GTR + I + Γ). In MrBayes, each analysis consisted of two four-chained MCMC runs for 100 million generations, with sampling of model parameters occurring every 1,000 generations. The initial 10% of generations were discarded as burin. The program Tracer v.1.7.1 (Rambaut et al. 2018) was used to verify whether the two independent MCMC runs of each analysis had converged and whether the model parameters had reached and remained at the stationary phase. Majority-rule consensus trees were then annotated in FigTree v.1.4.4 (Rambaut 2016).

Results

Taxonomy

Encyrtus eulecaniumiae Wang & Zhang

Encyrtus eulecaniumiae Wang & Zhang in Wang et al. (2016) (*nomen nudum*)

Diagnosis. *Encyrtus eulecaniumiae* can be morphologically differentiated from its closest allies by having the 2nd outer plate at least 0.65× as long as the ovipositor shield (2nd outer plate less than 0.60× as long as the ovipositor shield in both *E. sasakii* and

E. rhodococcusiae). *Encyrtus eulecaniumiae* can be further distinguished from *E. rhodococcusiae* by its shallowly concave hypopygium (hypopygium deeply concave in *E. rhodococcusiae*). According to Wang et al. (2016), *E. eulecaniumiae* is molecularly distinct from both *E. sasakii* and *E. rhodococcusiae* in having the following nucleotides in the COI marker (according to Wang et al. 2016): 14 (A), 47 (G), 53 (G), 68 (G), 134 (A), 203 (G), 236 (G), 266 (G), 271 (G), 281 (A), 341 (A), 461 (A), 470 (A) and 533 (A). *Encyrtus eulecaniumiae* is also unique ecologically by being the only one to attack the coccids *Eulecanium kuwanai* Kanda and *E. giganteum* Shinji.

Description. (reproduced from Wang et al. 2016) Female – Length about 3 mm including ovipositor sheaths. *Colouration*: Head black around ocellar area, anterior ocellus to top of scrobe pale brownish yellow to black, malar space brown; face largely brownish yellow; radicle pale orange to brown; scape mostly pale brown (Wang et al. 2016: fig. 6a); pedicel dark brown to black; funicular segments black; clava black; pronotum dorsally dark brown, laterally pale brown; thorax covered with dark brown setae, mesoscutum mostly black dorsally, laterally brown; scutellum black with a broad transverse yellow band and tuft of black bristles apically; metanotum black; tegula brown; mesopleuron pale brown; fore and hind coxae brownish yellow; mid coxa mostly brown; legs otherwise brown; basal one third of forewing hyaline, infuscate elsewhere; forewing with a series of long bristles just below the apical third of submarginal; propodeum brown dorsally, yellowish brown laterally; gaster black; ovipositor sheaths yellow, except apical one-third dark brown (Wang et al. 2016: fig. 6b). *Head*: Frontovertex about half the head width; ocelli forming an obtuse angle (about ~120°); scrobal depression ∩-shaped in frontal view; eye at least superficially bare; torulus separated from mouth margin by about one of its own length; toruli separated from each other by about 4× their own diameter. Antenna (Wang et al. 2016: fig. 6a) 13-segmented, scape cylindrical, 4.5× as long as broad; F1 about 1.4× longer than wide, F2 a little longer than wide, F3 and F4 as long as wide, F5 and F6 a little wider than long; clava short and 3-segmented; clypeus with three to six long, suberect setae; maxillary and labial palpi with 4 and 3 segments respectively. *Thorax*: Pronotum about one-sixth of mesoscutum length in dorsal view, with surface sloping from posterior margin, uniformly setose and fine reticulate sculpture. Mesoscutum 1.47× wider than long; uniformly convex, setose and finely reticulated, without notauli. Scutellum with a tuft of black bristles apically. Side of propodeum nearly bare below spiracle, but with a few inconspicuous setae on posterior margin above hind coxa; mesotibia with strong setae apically, without differentiated rows of spines; mesotibial spur about 1.7× as long as apical width of tibia (Wang et al. 2016: fig. 6e); mid basitarsus about 2× as long as wide and nearly as long as remaining segments. Forewing (Wang et al. 2016: fig. 6c) hyaline proximally, distinctly infuscate on apical two thirds; stigmal vein apically curved. *Gaster*: broadly sessile, with seven visible, uniformly gastral tergites; hypopygium almost reaching apex of gaster.

Type material. (reproduced from Wang et al. 2016)**:** ***Holotype*** – ♀, specimen E4-306A, China, Beijing, Shijingshan (Badachu Park), 15.V.2014, col. Ying Wang, ex. *Eulecanium kuwanai* on *Ulmus pumila* (deposited in IZCAS). ***Paratypes*** – 2♀♀, Chi-

na, Beijing, Shijingshan (Badachu Park), 15.V.2014, col. Ying Wang, ex. *Eulecanium kuwanai* on *Ulmus pumila* (deposited in IZCAS); 4♀♀ 2♂♂, China, Heilongjiang, Harbin, 9.VI.2011, col. Ying Wang, ex. *Eulecanium kuwanai* on

Ulmus pumila (deposited in IZCAS); 16♀♀ 5♂♂, China, Henan, Zhengzhou, 4.V.2007, col. Xiong Wang, ex. *Eulecanium kuwanai* on *Sophora japonica* (deposited in IZCAS); 221♀♀ 72♂♂, China, Inner Mongolia, Hohhot, 26.V.2012, col. Haibin Li, ex. *Encyrtus giganteum* on *Sophora japonica* (deposited in IZCAS); 62♀♀ 40♂♂, Shanxi, Taiyuan, 1.V.2007, col. Jie Li, ex. *Eulecanium kuwanai* on *Siophora japonica* (deposited in IZCAS); 85♀♀ 33♂♂, China, Shandong, Taian, 11.V.2008, col. Yanzhou Zhang, ex. *Eulecanium kuwanai* on *Sophora japonica* (deposited in IZCAS).

Encyrtus rhodococcusiae Wang & Zhang

Encyrtus rhodococcusiae Wang & Zhang in Wang et al. (2016) (*nomen nudum*)

Diagnosis. *Encyrtus rhodococcusiae* can be diagnosed morphologically within the *E. sasakii* complex through the combination of the 2nd outer plate less than 0.6× as long as the ovipositor shield (2nd outer plate at least 0.65× as long as the ovipositor shield in *E. eulecaniumiae*) and hypopygium deeply concave (hypopygium shallowly concave in *E. sasakii*). *Encyrtus rhodococcusiae* can be further differentiated from *E. sasakii* by having the ventral surface of the clava more than 1.5× as long as the dorsal one (in *E. sasakii*, the ventral surface of the clava is always less than 1.5× as long as the dorsal one). According to Wang et al. (2016), *E. rhodococcusiae* can be molecularly distinguished from its closest allies (*E. sasakii* and *E. eulecaniumiae*) by having the following nucleotides in the COI marker: 14 (T), 26 (A), 102 (A), 149 (A), 161 (C), 176 (G), 215 (G), 266 (T), 269 (A), 281 (T), 389 (A), 446 (A), 468 (C), 470 (T) 521 (T) and 530 (G). *Encyrtus rhodococcusiae* is also unique within the *E. sasakii* complex in attacking the coccid species *Rhodococcus sariuoni* Borchsenius.

Description. (reproduced from Wang et al. 2016) Female – Length including ovipositor 1.9 mm. *Colouration*: Head black around ocellar area, frontovertex black; malar space brown; antenna with scape yellowish brown; pedicel and flagellum dark brown; maxillary and labial palpi yellowish brown; pronotum dark brown to black dorsally, laterally pale brown; thorax covered with dark-brown setae; mesoscutum mostly black dorsally, laterally brown; sctuellum black with a broad transverse yellow band and a tuft of black bristles apically; metanotum dark brown; tegula dark brown; mesopleuron pale brown; fore and hind coxae brownish yellow (Wang et al. 2016: fig. 7d, f); mid coxa mostly brown (Wang et al. 2016: fig. 7e); legs otherwise dark brown; basal one third of forewing hyaline, infuscate elsewhere; forewing with a series of long bristles just below the apical third of submarginal; propodeum brown dorsally, yellowish brown laterally; gaster black; ovipositor sheaths yellow, except apex one-third dark brown (Wang et al. 2016: fig. 7b). *Head*: frontovertex about half the head width; ocelli forming an obtuse angle (~120°); scrobes quite shallow and ∩-shaped in frontal view;

eye at least superficially bare; torulus separated from mouth margin by about one of its own length; toruli separated from each other by about 2.5× their own diameter; antenna with scape subcylindrical, 3.4× as long as broad; pedicel subtriangular, 1.4× as long as broad and as broad as scape. Antenna (Wang et al. 2016: fig. 7a) 13-segmented, scape cylindrical; clava 3-segmented, its apex distinctly truncate; mandible plow shaped; clypeus with three to six conspicuous, long, suberect setae; maxillary and labial palpi with 4 and 3 segments respectively. *Thorax*: Mesoscutum 1.44× wider than long, uniformly convex, setose and finely reticulated, without notauli. Pronotum very short, about one eleventh the mesoscutum length, with polygonal reticulation; scutellum about 1.2× as long as broad, sculpture anteriorly similar to that of mesoscutum; forewing (Wang et al. 2016: fig. 7c) about 2.3× as long as broad; costal cell with more than one line of setae dorsally; stigma vein apically curved. *Gaster*: Hypopygium almost reaching apex of gaster.

Type material. (reproduced from Wang et al. 2016) ***Holotype*** – ♀, specimen 11-009A, China, Shandong, Linyi, 9.V.2011, col. Xuemei Yang, ex. *Rhodococcus sariuoni* on *Crataegus pinnatifida* (deposited in IZCAS). ***Paratypes*** – 2♀♀, China, Beijing, Haidian, 15.V2006, col. Yanzhou Zhang, ex. *Rhodococcus sariuoni* on *Malus spectabilis* (deposited in IZCAS); 3♀♀, China, Heilongjiang, Harbin, 15.VI.2007, col. Yanzhou Zhang, ex. *Rhodococcus sariuoni* on *Prunus persica* (deposited in IZCAS); 6♀♀ 1♂, China, Jilin, Changchun, 9.VI.2011, col. Ying Wang, ex. *Rhodococcus sariuoni* on *Prunus persica* (deposited in IZCAS); 2♀♀ 2♂♂, China, Qinghai, Xining, 28.VI.2013, col. Haibin Li, Xubo Wang, Xu Zhang, ex. *Rhodococcus sariuoni* on *Prunus cerasifera* (deposited in IZCAS); 7♀♀ 2♂♂, China, Shandong, Taian, 9.V.2008, col. Yanzhou Zhang, ex. *Rhodococcus sariuoni* on *Prunus cerasifera* (deposited in IZCAS); 2♀♀, China, Shaanxi, Xianyang, 9.V.2011, col. Feng Yuan, ex. *Rhodococcus sariuoni* on *Malus sieversii* (deposited in IZCAS).

Morphometry

Antenna: Our ANOVA analyses show that the LW ratios of both surfaces of C1 plus C2 are statistically different ($p < 0.001$ in both analyses) among *E. eulecaniumiae*, *E. rhodococcusiae* and *E. sasakii*. Linear regressions of the LW ratios of both C1 and C2 also differ ($p < 0.05$ in both) among species, even though the two ratios are significantly correlated when phylogenetic constraints are enforced ($p < 0.001$). Linear regression between the dorsal length and width of the clava also shows significant statistical difference among the three species ($p < 0.05$). We found further significant differences between *E. eulecaniumiae* and *E. rhodococcusiae* in the LW ratios of the ventral and dorsal surfaces of C1 ($p < 0.05$ in both) as well as in the dorsal lengths of both C1 and C2 ($p < 0.001$ and $p < 0.05$, respectively). In turn, the width of C2 is statistically different between *E. sasakii* and *E. eulecaniumiae* ($p < 0.05$).

Our analyses revealed that the LW ratio of the funicle is statistically different among the three species ($p < 0.05$) and positively correlated with the total length of antenna ($p < 0.001$). The LW ratios of F1, F3 and F5 are each separately correlated

with the total length of antenna as well ($p < 0.001$ in all analyses). Also, the lengths and widths of all funicular antennomeres are positively allometric (allometry coefficients 1.7–2.0). Linear regressions, however, show that these relationships are not species-specific ($p = 0.05–0.1$).

Ovipositor: The lengths of all analysed components of the ovipositor are significantly different between pairs of species, even though none of them separates all three species (see Suppl. material 1: Table S3). On the other hand, the length ratio between the 1st and 2nd outer plates ($p < 0.001$) as well as that between the lengths of the 2nd outer plate and shield of the ovipositor ($p < 0.001$) are both significantly different among the three species. Our analyses also show that (i) the length ratio between the two outer plates is significantly correlated with the length of the ovipositor shield ($p < 0.001$); (ii) the relationship between length and width is positively allometric in both the stylus and 2nd outer plate of the ovipositor, slopes 1.67 ($p < 0.001$) and 2.5 ($p < 0.001$), respectively; and (iii) the lengths of the stylus and ovipositor shield are also allometric (slope 2.0, $p < 0.001$). None of these results, however, shows species separation.

Among the analysed components of the ovipositor, the shape (EPC1) of the shield differs significantly among the three species ($p < 0.001$). The shapes of the two outer plates, however, differ only between *E. rhodococcusiae* and the other two species ($p < 0.01$), although linear regression of the shape parameters of the 2nd outer plate provides statistical difference among all species ($p < 0.05$). According to EPC1, the shapes of the two outer plates of the ovipositor are correlated with each other ($p < 0.005$), as is the shape of the ovipositor shield and its total length ($p < 0.001$), in all three species.

Hypopygium: PC2 of hypopygium shape shows clear separation among all three species ($p < 0.001$). In all of them, the shape of the hypopygium (PC1) is allometric in relation to its barycenter size (ordinary correlation: $p < 0.001$, evolutionary correlation: $p < 0.05$). Regression between hypopygium shape (PC1) and length of ovipositor shield shows difference among the species ($p < 0.05$). Both EPC1 and EPC2 indicate that the shape parameters of the hypopygium are correlated with forewing length ($p < 0.05$ and $p < 0.001$, respectively).

Correlations between structures: The lengths of the antenna, hypopygium and all the components of the ovipositor are negatively allometric to forewing length ($p < 0.001$). In turn, the forewing length is positively correlated with the LW ratio of clava ($p < 0.001$) as well as with EPC1 of the shapes of ovipositor shield and 2nd outer plate ($p < 0.001$ and $p < 0.05$, respectively). The total length of antenna and ventral length of C2 are independently positively correlated with EPC2 of the hypopygium shape ($p < 0.001$ and $p < 0.05$, respectively). The average LW ratio of the ventral surface of C1 plus C2 is strongly correlated with the shape (EPC1) of the 2nd outer plate of the ovipositor ($p < 0.001$). EPC1 of the shapes of the hypopygium and ovipositor shield are also correlated to each other ($p < 0.05$).

Phylogenetic analysis: The majority-rule consensus trees obtained through the Bayesian analysis of the combined dataset, as well as those of the 28S and COI datasets only, are shown in Figs 3, S1, S2, respectively. The two latter trees show that each of the three species belonging to the *E. sasakii* complex forms a monophyletic group,

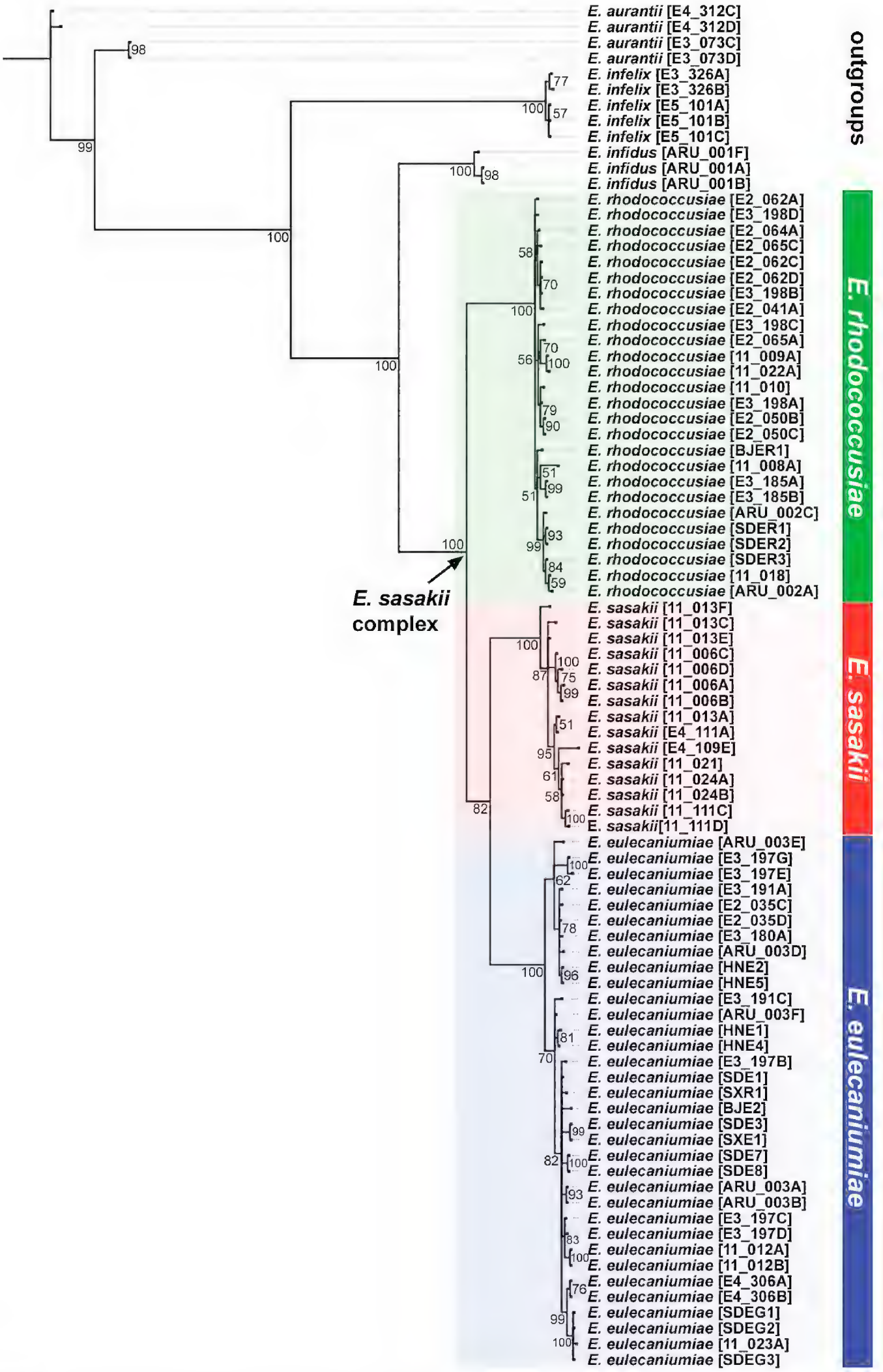

Figure 3. Phylogenetic tree of the *Encyrtus sasakii* species complex obtained through Bayesian analysis of the combined molecular dataset (COI plus 28S). Numbers at internodes are posterior probabilities of corresponding clades.

all with 100% posterior probability support (henceforth PP). The clade linking the three species (i.e., the *E. sasakii* complex itself) is also maximally supported by the COI and multilocus analyses. Both further reveal that *E. rhodococcusiae* is sister to *E. eulecaniumiae* plus *E. sasakii*, even though the sister-group relationship between the two latter species is only weakly supported (COI = 53% PP, multilocus = 82% PP).

On the other hand, the Bayesian analysis of 28S alone yields a considerably different phylogenetic scenario. *Encyrtus rhodococcusiae* is retrieved as more closely related to *E. infidus* than to the other two species, and it also renders *E. sasakii* paraphyletic. In fact, *E. rhodococcusiae* is the only one of the three species to form a monophyletic group, albeit with weak support (80% PP). All terminals of *E. sasakii* most likely have identical 28S sequences in terms of nucleotide composition, except specimens 11_111D and 11_013C which are recovered as more closely related to *E. rhodococcusiae* and *E. eulecaniumiae*, respectively, an arrangement that renders *E. sasakii* polyphyletic. The clade nesting all *E. eulecaniumiae* is relatively strongly supported (96% PP), but the species is made paraphyletic due to the placement of a single terminal of *E. sasakii* (11_013C).

Discussion

Taxonomic problem regarding *E. eulecaniumiae* and *E. rhodococcusiae*

The descriptions of *E. eulecaniumiae* and *E. rhodococcusiae* by Wang & Zhang in Wang et al. (2016), which appeared in the first issue of the sixth volume of the electronic-only *Scientific Reports*, are unfortunately invalid because the work does not qualify as published according to the International Code of Zoological Nomenclature (hereafter 'the Code'; ICZN 1999). This is because the journal failed to provide evidence that the work (or the new names erected therein) had been registered in the Official Register of Zoological Nomenclature (ZooBank) (see Article 8.5). Consequently, both *E. eulecaniumiae* and *E. rhodococcusiae* are currently *nomina nuda*. The Code is explicit in determining that not only the registrations in ZooBank must be done, but also that the works must themselves contain evidence of such registrations (Article 8.5.3). The latter requirement has typically been fulfilled by simply providing the unique registration number that is assigned to each new entry in ZooBank. Since both parasitoid species remain technically unnamed, we herein validate their descriptions under the same names chosen by the original authors.

Integrative taxonomy

It took nearly a century for hymenopterists to realize that what has always thought to be a single parasitoid species (*E. sasakii*) could, in fact, constitute a complex of three cryptic species. The first clue came through DNA barcoding of laboratory-reared individuals, which revealed unexpectedly high intraspecific genetic variation in the COI

locus (Chesters et al. 2012). In a subsequent publication, two cryptic species (*E. eulecaniumiae* and *E. rhodococcusiae*) were described based on host preferences and molecular data, even though the authors could not find any reliable morphological feature to permit distinction of the three species (Wang et al. 2016). This motivated us to reassess the taxonomic status of the *E. sasakii* complex through an integrative approach, performing Bayesian analyses of previously-available and newly-sequenced molecular data (COI and 28S) plus morphometric analyses of several functional morphological traits – antenna, ovipositor and hypopygium. While previous authors have focused on relative size of the antenna and/or ovipositor (Sugonjaev and Gordh 1982; Chesters et al. 2012; Wang et al. 2016), shape analyses of both the ovipositor and hypopygium are, to our knowledge, novel for *Encyrtus*. Although most of our analyses yielded non-significant results (as Fontaneto et al. 2007), many supported statistically the separation of either pairs of species or among all three species.

We herein demonstrate through ANOVA and linear regression analyses that the LW ratios of several antennal subunits are statistically different among the three *Encyrtus* species. As opposed to analysing the clava solely as a single structure, as previously done (Wang et al. 2016), we took a step forward and also performed separate analyses with each of its constituent antennomeres (C1–C3) aiming for a more comprehensive approach (as in Kim and Jang 2012). In fact, the analyses of C1 and C2 (when taken both individually and in combination) yielded the strongest evidence provided herein for the existence of three cryptic species within the *E. sasakii* complex, while those of C3 did not show any species separation. Previously, Wang et al. (2016) found significant differences in the total width of the clava separating only *E. eulecaniumiae* from the other two species. Analyses performed herein also found significant differences in the LW ratio of the funicle among the three *Encyrtus* species, but not in any of its constituent antennomeres (F1–F6) separately, despite previous analyses have found the widths of F3 and F5 to be statistically different among the species (Wang et al. 2016).

It appears, therefore, that the claval antennomeres evolve rather independently among themselves, but not the funicular ones, which is interesting since the former is comprised by three nearly-fused antennomeres while the latter by six that are more freely articulated. Since the LW ratios of the funicle, C1 and C2 are all statistically uncorrelated with the total length of the antenna (as well as with that of the forewing), it is possible to conclude that they are positively allometric in growth within the *E. sasakii* complex. More specifically, the longer the antenna, the longer is the funicle in relation to the clava (or, conversely, the broader is the clava in relation to the funicle). This shifts the general shape of the antenna, generally speaking, from 'more cylindrical' to 'more conical'. Elongation of the antenna in parasitoids has been suggested to be evolutionarily associated with the mechanism of host detection (Polaszek et al. 2004).

As done with the antenna, we analysed the main structural components of the ovipositor separately seeking for a higher amount of morphometric evidence. This led us to find out that the relative length of the 2nd outer plate and those of both the 1st outer plate and shield are statistically different among all three species within the *E. sasakii* complex. It was previously known that the total length of the stylus differs significantly

between *E. eulecaniumiae* and the other two species (Wang et al. 2016). Of particular relevance was the finding that the 2nd outer plate is allometric in relation to the shield, although this result was largely caused by two individuals of *E. sasakii* (nj_ta_002 and 11_006C) with exceptionally long ovipositors; when both are excluded from the analysis, the slope is not different from 1 (95% interval: 0.893–1.511) and thus allometry is not observed. Our analyses also showed, for the first time, that the shape of the hypopygium is significantly different among the three species; this difference, however, was only explained by PC2. Unfortunately, there was not enough data for us to perform an EPC analysis with the hypopygium.

Phylogenetic relationships and biogeography

The analysis of our combined molecular dataset resulted in a phylogenetic tree that provides strong additional support for there being three distinct species within the *E. sasakii* complex (Fig. 3). The analysis of the 28S data alone, on the other hand, yielded a largely unresolved tree (Suppl. material 1: Fig. S1), which is actually not surprising given the rather slow-evolving nature of the marker (Zardoya et al. 1998; Foighil and Taylor 2000; Razak et al. 2019). We nonetheless found more divergence in terms of nucleotide composition in 28S than Wang et al. (2016) did previously, although a plausible explanation would simply be that more comprehensive DNA datasets (30 of the 87 sequences employed by us were new) are more likely to encompass larger divergences. Even small degrees of divergence in a well conserved marker, such as the 28S, may provide new insights for taxonomically challenging groups (Gebiola et al. 2010). Unfortunately, Wang et al. (2016) did not construct a tree based exclusively on their 28S data, which prevented us from making a direct comparison of phylogenetic results. However, it is possible to assert that the relationships recovered through our 28S analysis were distinct from those of both combined (Fig. 3) and COI (Suppl. material 1: Fig. S2) analyses, once again, a common outcome in many studies of hymenopterans (e.g., Almeida et al. 2019; Ferrari et al. 2020). A quite unexpected result, in particular, was the placement of one *E. sasakii* terminal (11-013C) in the comb containing all *E. eulecaniumiae*. This finding may be seen as an indication of a recent hybridisation between the two species (Agatsuma et al. 2000; Funk and Omland 2003), although we unfortunately cannot rule out a contamination since we were not able to validate the molecular work done previously (see Wang et al. 2016).

Rather than analysing our data through phenetic methods (such as neighbor-joining) as commonly done by species-delimitation studies of hymenopterans (e.g. Ross and Shoemaker 2005; Dong et al. 2018; Triapitsyn et al. 2020), we opted for a Bayesian approach, which has broadly been recognized as scientifically more rigorous than the former (see King and Rücklin 2020). This likely led us to obtain a different result, according to which *E. sasakii* is phylogenetically closer to *E. eulecaniumiae* (hypothesis 1; see Figs 3, S2) than to *E. rhodococcusiae* (hypothesis 2; see Wang et al. 2016: fig. 5). It should be noted, however, that the clade uniting *E. sasakii* plus *E. eulecaniumiae* in our combined phylogeny is only weakly supported (PP 82%), which indicates that

future analyses of more comprehensive datasets are desirable. Nonetheless, the sister-species relationship between *E. sasakii* and *E. eulecaniumiae* is further supported by the general shape of the outer plates of their ovipositors, which exhibit less sharped corners than those of *E. rhodococcusiae*, as reflected in the significant differences found in the corresponding EPC1s.

A third possibility (hypothesis 3) – *E. eulecaniumiae* and *E. rhodococcusiae* as sister species – would make more sense on biogeographical grounds given that both are sympatrically distributed but allopatric to *E. sasakii* (Wang et al. 2016). Based on this scenario, a vicariant event would have separated *E. sasakii* from the ancestor of the other two species, which would have then undergone sympatric speciation. Hypothesis 3 can be further defended in light of the available host-use data, since the known hosts of *E. eulecaniumiae* (*Eulecanium kuwanai* and *Eulecanium giganteum*) and *E. rhodococcusiae* (*Rhodococcus sariuoni*) are phylogenetically closer to each other than to that of *E. sasakii*, *Takahashia japonica* (Cockerell) (Choi and Lee 2019). Thus, diversification would have occurred primarily due to parasitoid-host cospeciation (i.e., concomitant divergence of host and parasite taxa; see Brooks 1979). However, documented instances of cospeciation across the animal kingdom are much rarer than other natural phenomena, such as duplication and host shift (Brooks and McLennan 1993). In fact, host shift has been indicated as the most probable cause of topological incongruence between parasite-host phylogenies (De Vienne et al. 2013; Onuferko et al. 2019), and likely also explains the case reported in this paper.

Conclusions

Both the morphometric and molecular evidences provided in this paper confirm that the three cryptic species of parasitoid wasps must be recognized within the *E. sasakii* complex. However, all interspecific morphological differences listed herein can be detected only statistically, which means that none of the three species can be readily diagnosed morphologically. We nonetheless validated the use of shape morphometric analyses as a reliable approach to species delimitation within Hymenoptera, especially when combined with other lines of evidence.

Our phylogeny recovered *E. sasakii* and *E. eulecaniumiae* as sister species, a hypothesis that has not yet been raised; but because the clade uniting the two species is only weakly supported by our molecular dataset, we encourage a reappraisal of this controversy in the future.

Acknowledgements

This work was supported by the National Natural Science Foundation of China under Grant (No.31872269), the National Science Fund for Distinguished Young Scholars (grant number 31625024); the President's International Funding Initiative (grant

numbers 2018PB0007 and 2020PB0130) to AR and RRF, respectively. RRF was further supported by the National Natural Science Foundation of China (grant number 41761144068). We thank Mei Xiong (Institute of Zoology, Chinese Academy of Sciences) for the help with the preparation of the parasitoid specimens, and Dr. Michael Orr (Institute of Zoology, Chinese Academy of Sciences) provided constructive comments on this manuscript. Author contributions: AR, CDZ, and YZZ (conceptualization), AR and RF (methodology), AR and YZZ (investigation), AR, RF, CDZ and YZZ (writing, review and editing), CDZ and YZZ (supervision), and AR, RF, CDZ and YZZ (funding acquisition). All authors have read and agreed to the published version of the manuscript.

References

Agatsuma T, Arakawa Y, Iwagami M, Honzako Y, Cahyaningsih U, Kang SY, Hong SJ (2000) Molecular evidence of natural hybridization between *Fasciola hepatica* and *F. gigantica*. Parasitology International 49: 231–238. https://doi.org/10.1016/S1383-5769(00)00051-9

Allemand R (1982) Physiological tolerance of *Drosophila simulans* to dark environment: A comparison with *D. melanogaster*. Journal of Insect Physiology 28: 767–772. https://doi.org/10.1016/0022-1910(82)90137-8

Almeida EAB, Packer L, Melo GAR, Danforth BN, Cardinal SC, Quinteiro FB, Pie MR (2019) The diversification of neopasiphaeine bees during the Cenozoic (Hymenoptera: Colletidae). Zoologica Scripta 48: 226–242. https://doi.org/10.1111/zsc.12333

Amato A, Kooistra WH, Ghiron JHL, Mann DG, Pröschold T, Montresor M (2007) Reproductive isolation among sympatric cryptic species in marine diatoms. Protist 158: 193–207. https://doi.org/10.1016/j.protis.2006.10.001

Arbuthnott D, Crespi BJ (2009) Courtship and mate discrimination within and between species of *Timema* walking-sticks. Animal Behaviour 78: 53–59. https://doi.org/10.1016/j.anbehav.2009.02.028

Broad GR, Quicke DL (2000) The adaptive significance of host location by vibrational sounding in parasitoid wasps. Proceedings of the Royal Society of London. Series B: Biological Sciences 267: 2403–2409. https://doi.org/10.1098/rspb.2000.1298

Brooks DR (1979) Testing the context and extent of host-parasite coevolution. Systematic Biology 28: 299–307. https://doi.org/10.1093/sysbio/28.3.299

Brooks DR, McLennan DA (1993) Parascript: Parasites and the language of evolution. Smithsonian series in comparative evolutionary biology (USA).

Chesters D, Wang Y, Yu F, Bai M, Zhang TX, Hu HY, Zhu CD, Li CD, Zhang YZ (2012) The integrative taxonomic approach reveals host specific species in an encyrtid parasitoid species complex. PLoS ONE 7: e37655. https://doi.org/10.1371/journal.pone.0037655

Choi J, Lee S (2020) Molecular phylogeny of the family Coccidae (Hemiptera, Coccomorpha), with a discussion of their waxy ovisacs. Systematic Entomology 45: 396–414. https://doi.org/10.1111/syen.12404

De Vienne D, Refrégier G, López-Villavicencio M, Tellier A, Hood ME, Giraud T (2013) Cospeciation vs host-shift speciation: methods for testing, evidence from natural associations and relation to coevolution. New Phytologist 198: 347–385. https://doi.org/10.1111/nph.12150

Delicado D, Arconada B, Aguado A, Ramos MA (2019) Multilocus phylogeny, species delimitation and biogeography of Iberian valvatiform springsnails (Caenogastropoda: Hydrobiidae), with the description of a new genus. Zoological Journal of the Linnean Society 186: 892–914. https://doi.org/10.1093/zoolinnean/zly093

Dépraz A, Hausser J, Pfenninger M (2009) A species delimitation approach in the *Trochulus sericeus/hispidus* complex reveals two cryptic species within a sharp contact zone. BMC Evolutionary Biology 9: 1–10. https://doi.org/10.1186/1471-2148-9-171

Desneux N, Blahnik R, Delebecque CJ, Heimpel GE (2012) Host phylogeny and specialisation in parasitoids. Ecology Letters 15: 453–460. https://doi.org/10.1111/j.1461-0248.2012.01754.x

DeVries PJ, Penz CM, Hill RI (2010) Vertical distribution, flight behaviour and evolution of wing morphology in *Morpho* butterflies. Journal of Animal Ecology 79: 1077–1085. https://doi.org/10.1111/j.1365-2656.2010.01710.x

Dincă V, Montagud S, Talavera G, Hernández-Roldán J, Munguira ML, García-Barros E, Hebert PDN, Vila R (2015) DNA barcode reference library for Iberian butterflies enables a continental-scale preview of potential cryptic diversity. Scientific Reports 5: 1–12. https://doi.org/10.1038/srep12395

Dong Z, Liu S, Zhang Z (2018) Efficacy of using DNA barcoding to identify parasitoid wasps of the melon-cotton aphid (*Aphis gossypii*) in watermelon cropping system. BioControl 63: 677–685. https://doi.org/10.1007/s10526-018-9894-4

Fea MP, Mark CJ, Holwell GI (2019) Sexually dimorphic antennal structures of New Zealand cave wētā (Orthoptera: Rhaphidophoridae). New Zealand Journal of Zoology 46: 124–148. https://doi.org/10.1080/03014223.2018.1520266

Ferrari RR, Onuferko TM, Monckton SK, Packer L (2020) The evolutionary history of the cellophane bee genus *Colletes* Latreille (Hymenoptera: Colletidae): molecular phylogeny, biogeography and implications for a global infrageneric classification. Molecular Phylogenetics and Evolution 146: e106750. https://doi.org/10.1016/j.ympev.2020.106750

Foighil DO, Taylor DJ (2000) Evolution of parental care and ovulation behavior in oysters. Molecular Phylogenetics and Evolution 15: 301–313. https://doi.org/10.1006/mpev.1999.0755

Fontaneto D, Giordani I, Melone G, Serra M (2007) Disentangling the morphological stasis in two rotifer species of the *Brachionus plicatilis* species complex. Hydrobiologia 583: 297–307. https://doi.org/10.1007/s10750-007-0573-1

Fox J (2005) Getting started with the R commander: a basic-statistics graphical user interface to R. Journal of Statistical Software 14: 1–42. https://doi.org/10.18637/jss.v014.i09

Frankino WA, Zwaan BJ, Stern DL, Brakefield PM (2007) Internal and external constraints in the evolution of morphological allometries in a butterfly. Evolution: International Journal of Organic Evolution 61: 2958–2970. https://doi.org/10.1111/j.1558-5646.2007.00249.x

Funk DJ, Omland KE (2003) Species-level paraphyly and polyphyly: frequency, causes, and consequences, with insights from animal mitochondrial DNA. Annual Review of Ecology, Evolution, and Systematics 34: 397–423. https://doi.org/10.1146/annurev.ecolsys.34.011802.132421

Gebiola M, Bernardo U, Burks R (2010) A reevaluation of the generic limits of *Pnigalio* Schrank (Hymenoptera: Eulophidae) based on molecular and morphological evidence. Zootaxa 2484: 35–44. https://doi.org/10.11646/zootaxa.2484.1.3

Ghara M, Kundanati L, Borges RM (2011) Nature's Swiss Army knives: ovipositor structure mirrors ecology in a multitrophic fig wasp community. PLoS ONE 6: e23642. https://doi.org/10.1371/journal.pone.0023642

Gokhman VE (2018) Integrative taxonomy and its implications for species-level systematics of parasitoid Hymenoptera. Entomological Review 98: 834–864. https://doi.org/10.1134/S0013873818070059

Gutiérrez-Valencia J, Gutiérrez Y, G Dias L (2017) Species delimitation in the crypsis-defended and polymorphic stick insects of the genus *Libethra* (Phasmatodea, Diapheromeridae). Zoologica Scripta 46: 693–705. https://doi.org/10.1111/zsc.12242

Hall T (1999) BioEdit: a user-friendly biological sequence alignment editor and analysis program for Windows 95/98/NT. In Nucleic Acids Symposium Series 41: 95–98.

Hammer Ø, Harper DAT, Ryan PD (2001) PAST: Paleontological statistics software package for education and data analysis. Palaeontologia Electronica 4: 9–18.

Hansson C, Schmidt S (2020) A revision of European species of the genus *Tetrastichus* Haliday (Hymenoptera: Eulophidae) using integrative taxonomy. Biodiversity Data Journal 8: e59177. https://doi.org/10.3897/BDJ.8.e59177

Huelsenbeck JP, Ronquist F (2001) MRBAYES: Bayesian inference of phylogeny. Bioinformatics 17: 754–755. https://doi.org/10.1093/bioinformatics/17.8.754

Kim H, Jang Y (2012) Taxonomic review and morphometric analysis of the genus *Melanaphis* van der Goot (Hemiptera: Aphididae) in Korea. Animal Cells and Systems 16: 34–40. https://doi.org/10.1080/19768354.2011.620621

King B, Rücklin M (2020) A Bayesian approach to dynamic homology of morphological characters and the ancestral phenotype of jawed vertebrates. Elife 9: e62374. https://doi.org/10.7554/eLife.62374

International Commission on Zoological Nomenclature (1999) International Code of Zoological Nomenclature. 4th edn. The International Trust for Zoological Nomenclature (Padova): 1–306.

Ishii T (1928) The Encyrtidae of Japan. I. Bulletin of the Imperial Agricultural Experiment Station of Japan 3: 79–160.

Klingenberg CP, Zimmermann M (1992) Static, ontogenetic, and evolutionary allometry: a multivariate comparison in nine species of water striders. The American Naturalist 140: 601–620. https://doi.org/10.1086/285430

Krishnan A, Sane SP (2015) Antennal mechanosensors and their evolutionary antecedents. Advances in Insect Physiology 49: 59–99. https://doi.org/10.1016/bs.aiip.2015.06.003

Lanfear R, Frandsen PB, Wright AM, Senfeld T, Calcott B (2017) PartitionFinder 2: new methods for selecting partitioned models of evolution for molecular and morphological phylo-

genetic analyses. Molecular Biology and Evolution 34: 772–773. https://doi.org/10.1093/molbev/msw260

Lukhtanov VA (2019) Species delimitation and analysis of cryptic species diversity in the XXI century. Entomological Review 99: 463–472. https://doi.org/10.1134/S0013873819040055

Maddison WP, Maddison DR (2019) Mesquite: a modular system for evolutionary analysis. Version 3.6. http://mesquiteproject.org [Accessed on 08.01.2019]

Midford PE, Garland Jr T, Maddison WP (2019) PDAP: PDTREE package for Mesquite. Version 1.15. http://mesquiteproject.org/pdap_mesquite [Accessed on 08.01.2019]

Miller MA, Pfeiffer W, Schwartz T (2011) The CIPRES science gateway: a community resource for phylogenetic analyses. In: Proceedings of the 2011 TeraGrid Conference: extreme digital discovery. https://doi.org/10.1145/2016741.2016785

Milne M, Walter GH, Milne JR (2007) Mating behavior and species status of host-associated populations of the polyphagous thrips, *Frankliniella schultzei*. Journal of Insect Behavior 20: 331–346. https://doi.org/10.1007/s10905-007-9081-4

Monckton SK (2016) A revision of *Chilicola* (*Heteroediscelis*), a subgenus of xeromelissine bees (Hymenoptera, Colletidae) endemic to Chile: taxonomy, phylogeny, and biogeography, with descriptions of eight new species. ZooKeys 591: 1–144. https://doi.org/10.3897/zookeys.591.7731

Noyes JS (2010) Encyrtidae of Costa Rica (Hymenoptera: Chalcidoidea), 3. Subfamily Encyrtinae: Encyrtini, Echthroplexiellini, Discodini, Oobiini and Ixodiphagini, parasitoids associated with bugs (Hemiptera), insect eggs (Hemiptera, Lepidoptera, Coleoptera, Neuroptera) and ticks (Acari). Memoirs of the American Entomological Institute 84: 1–848.

Nugnes F, Bernardo U, Viggiani G (2017) An integrative approach to species discrimination in the *Anagrus atomus* group *sensu stricto* (Hymenoptera: Mymaridae), with a description of a new species. Systematics and Biodiversity 15: 582–599. https://doi.org/10.1080/14772000.2017.1299811

Onuferko TM, Bogusch P, Ferrari RR, Packer L (2019) Phylogeny and biogeography of the cleptoparasitic bee genus *Epeolus* (Hymenoptera: Apidae) and cophylogenetic analysis with its host bee genus *Colletes* (Hymenoptera: Colletidae). Molecular Phylogenetics and Evolution 141: e106603. https://doi.org/10.1016/j.ympev.2019.106603

Orr MC, Ascher JS, Bai M, Chesters D, Zhu CD (2020) Three questions: How can taxonomists survive and thrive worldwide? Megataxa 1: 19–27. https://doi.org/10.11646/megataxa.1.1.4

Padula V, Bahia J, Stöger I, Camacho-García Y, Malaquias MAE, Cervera JL, Schrödl M (2016) A test of color-based taxonomy in nudibranchs: Molecular phylogeny and species delimitation of the *Felimida clenchi* (Mollusca: Chromodorididae) species complex. Molecular Phylogenetics and Evolution 103: 215–229. https://doi.org/10.1016/j.ympev.2016.07.019

Polaszek A, Manzari S, Quicke DL (2004) Morphological and molecular taxonomic analysis of the *Encarsia meritoria* species-complex (Hymenoptera, Aphelinidae), parasitoids of whiteflies (Hemiptera, Aleyrodidae) of economic importance. Zoologica Scripta 33: 403–421. https://doi.org/10.1111/j.0300-3256.2004.00161.x

Pomfret JC, Knell RJ (2006) Sexual selection and horn allometry in the dung beetle *Euoniticellus intermedius*. Animal Behaviour 71: 567–576. https://doi.org/10.1016/j.anbehav.2005.05.023

Pramual P, Wongpakam K, Adler PH (2011) Cryptic biodiversity and phylogenetic relationships revealed by DNA barcoding of Oriental black flies in the subgenus *Gomphostilbia* (Diptera: Simuliidae). Genome 54: 1–9. https://doi.org/10.1139/G10-100

R Core Team (2019) R: A language and environment for statistical computing. R Foundation for Statistical Computing (Vienna). http://www.R-project.org/ [Accessed on 26.03.2019]

Rambaut A (2016) FigTree v.1.4.4. https://github.com/rambaut/figtree/releases

Rambaut A, Drummond AJ, Xie D, Baele G, Suchard MA (2018) Posterior summarization in Bayesian phylogenetics using Tracer 1.7. Systematic Biology 67: 901–904. https://doi.org/10.1093/sysbio/syy032

Razak NFA, Supramaniam CV, Zieritz A (2019) A dichotomous PCR-RFLP identification key for the freshwater mussels (Bivalvia: Unionida) of Peninsular Malaysia. Conservation Genetics Resources 11: 457–464. https://doi.org/10.1007/s12686-018-1038-8

Rohlf FJ (1990) Morphometrics. Annual Review of Ecology and Systematics 21: 299–316. https://doi.org/10.1146/annurev.es.21.110190.001503

Ronquist F, Teslenko M, Van Der Mark P, Ayres DL, Darling A, Höhn S, Larget B, Liu L, Suchard MA, Huelsenbeck JP (2012) MrBayes 3.2: efficient Bayesian phylogenetic inference and model choice across a large model space. Systematic Biology 61: 539–542. https://doi.org/10.1093/sysbio/sys029

Ross KG, Shoemaker DD (2005) Species delimitation in native South American fire ants. Molecular Ecology 14: 3419–3438. https://doi.org/10.1111/j.1365-294X.2005.02661.x

Rull J, Abraham S, Kovaleski A, Segura DF, Mendoza M, Liendo MC, Vera, MT (2013) Evolution of pre-zygotic and post-zygotic barriers to gene flow among three cryptic species within the *Anastrepha fraterculus* complex. Entomologia Experimentalis et Applicata 148: 213–222. https://doi.org/10.1111/eea.12094

Soto IM, Carreira VP, Fanara JJ, Hasson E (2007) Evolution of male genitalia: environmental and genetic factors affect genital morphology in two *Drosophila* sibling species and their hybrids. BMC Evolutionary Biology 7: 1–11. https://doi.org/10.1186/1471-2148-7-77

Sproul JS, Maddison DR (2017) Sequencing historical specimens: successful preparation of small specimens with low amounts of degraded DNA. Molecular Ecology Resources 17: 1183–1201. https://doi.org/10.1111/1755-0998.12660

Tan DS, Ang Y, Lim GS, Ismail MRB, Meier R (2010) From 'cryptic species' to integrative taxonomy: an iterative process involving DNA sequences, morphology, and behaviour leads to the resurrection of *Sepsis pyrrhosoma* (Sepsidae: Diptera). Zoologica Scripta 39: 51–61. https://doi.org/10.1111/j.1463-6409.2009.00408.x

Thompson JD, Higgins DG, Gibson TJ (1994) CLUSTAL W: improving the sensitivity of progressive multiple sequence alignment through sequence weighting, position-specific gap penalties and weight matrix choice. Nucleic Acids Research 22: 4673–4680. https://doi.org/10.1093/nar/22.22.4673

Triapitsyn SV, Rugman-Jones PF, Tretiakov PS, Daane KM, Wilson H (2020) Reassessment of molecular and morphological variation within the *Anagrus atomus* species complex (Hymenoptera: Mymaridae): egg parasitoids of leafhoppers (Hemiptera: Cicadellidae) in Europe and North America. Journal of Natural History 54: 1735–1758. https://doi.org/10.1080/00222933.2020.1827073

Trotta V, Pertoldi C, Rudoy A, Manenti T, Cavicchi S, Guerra D (2010) Thermal plasticity of wing size and shape in *Drosophila melanogaster*, *D. simulans* and their hybrids. Climate Research 43: 71–79. https://doi.org/10.3354/cr00880

Vodă R, Dapporto L, Dincă V, Vila R (2015) Why do cryptic species tend not to co-occur? A case study on two cryptic pairs of butterflies. PLoS ONE 10: e0117802. https://doi.org/10.1371/journal.pone.0117802

Qin YG, Zhou QS, Yu F, Wang XB, Wei JF, Zhu CD, Zhang YZ, Vogler AP (2018) Host specificity of parasitoids (Encyrtidae) toward armored scale insects (Diaspididae): Untangling the effect of cryptic species on quantitative food webs. Ecology and Evolution 8: 7879–7893. https://doi.org/10.1002/ece3.4344

Viggiani G (1999) Variations and biological traits of *Coccophagus gossypariae* Gahan (Hymenoptera: Aphelinidae). Biological Control 16: 43–46. https://doi.org/10.1006/bcon.1999.0735

Vinson SB (1998) The general host selection behavior of parasitoid Hymenoptera and a comparison of initial strategies utilized by larvaphagous and oophagous species. Biological Control 11: 79–96. https://doi.org/10.1006/bcon.1997.0601

Wang Y, Zhou QS, Qiao HJ, Zhang AB, Yu F, Wang XB, Zhu CD, Zhang YZ (2016) Formal nomenclature and description of cryptic species of the *Encyrtus sasakii* complex (Hymenoptera: Encyrtidae). Scientific Reports 6: 1–16. https://doi.org/10.1038/srep34372

Wiens JJ (2003) Missing data, incomplete taxa, and phylogenetic accuracy. Systematic Biology 52: 528–538. https://doi.org/10.1080/10635150390218330

Wonglersak R, Fenberg PB, Langdon PG, Brooks SJ, Price BW (2020) Temperature-body size responses in insects: a case study of British Odonata. Ecological Entomology 45: 795–805. https://doi.org/10.1111/een.12853

Zapata F, Jiménez I (2012) Species delimitation: inferring gaps in morphology across geography. Systematic Biology 61: 179–194. https://doi.org/10.1093/sysbio/syr084

Zardoya R, Cao Y, Hasegawa M, Meyer A (1998) Searching for the closest living relative(s) of tetrapods through evolutionary analyses of mitochondrial and nuclear data. Molecular Biology and Evolution 15: 506–517. https://doi.org/10.1093/oxfordjournals.molbev.a025950

Zhang YM, Gates MW, Shorthouse JD (2014) Testing species limits of Eurytomidae (Hymenoptera) associated with galls induced by Diplolepis (Hymenoptera: Cynipidae) in Canada using an integrative approach. The Canadian Entomologist 146: 321–334. https://doi.org/10.4039/tce.2013.70

Zhang YZ, Si SL, Zheng JT, Li HL, Fang Y, Zhu CD, Vogler AP (2011) DNA barcoding of endoparasitoid wasps in the genus *Anicetus* reveals high levels of host specificity (Hymenoptera: Encyrtidae). Biological Control 58: 182–191. https://doi.org/10.1016/j.biocontrol.2011.05.006

Zhou QS, Polaszek A, Qin YG, Yu F, Wang XB, Wu SA, Zhu CD, Zhang YZ, Pedata PA (2018) Parasitoid-host associations of the genus *Coccophagus* (Hymenoptera: Aphelinidae) in China. Zoological Journal of the Linnean Society 182: 38–49. https://doi.org/10.1093/zoolinnean/zlx019

Supplementary material 1

Tables and figures

Authors: Andrey Rudoy, Chao-Dong Zhu, Rafael R. Ferrari, Yan-Zhou Zhang

Data type: Tables and figures.

Explanation note: **Table S1** is mainly on information on the *Encyrtus* specimens used. **Table S2** includes loadings of the principal component (PC) analyses. **Table S3** includes P-values of the statistical analysesof variance (ANOVA) performed. **Figure S1** Bayesian tree of the Encyrtus sasakii complex obtained through analysis of the 28S sequence data only. **Figure S2** Bayesian tree of the Encyrtus sasakii complex obtained through analysis of the COI sequence data only.

Numbers at internodes are posterior probabilities of the corresponding clades.

Numbers at internodes are posterior probabilities of the corresponding clades.

Link: https://doi.org/10.3897/jhr.90.75807.suppl1